Supporting Information

Reliable and reusable whole-polypropylene plastic microfluidic devices for rapid, low-cost antimicrobial susceptibility test

Han Sun[a], Chiu-Wing Chan[a], Yisu Wang[a], Xiao Yao[a], Xuan Mu[*b], Xuedong Lu[c], Jianhua Zhou[d], Zongwei Cai[af], Kangning Ren[*,aef]

[a] Department of Chemistry, Hong Kong Baptist University. Waterloo Rd, Kowloon, Hong Kong, China.

[b] Department of Biomedical engineering, Tufts University, 4 colby, Medford, MA 02155, USA.

[c] Department of Laboratory Medicine, the Eighth Affiliated Hospital of Sun Yat-sen University, Shenzhen, China.

[d] Key Laboratory of Sensing Technology and Biomedical Instruments of Guangdong Province, Department of Biomedical Engineering, School of Engineering, Sun Yat-sen University, Guangzhou, China.

[e] HKBU Institute of Research and Continuing Education, Shenzhen, China.

[f] State Key Laboratory of Environmental and Biological Analysis, The Hong Kong Baptist University, Waterloo Rd, Kowloon, Hong Kong, China.

AUTHOR INFORMATION

Corresponding Author

* (K. N. Ren) Tel: (852) 34117067. E-mail: kangningren@hkbu.edu.hk.

*(X. Mu) Tel: 6178995339. E-mail: xuan.mu@tufts.edu.

ORCID

K. N. Ren: 0000-0002-8563-7654

X. Mu: 0000-0001-6692-2372

Present Addresses

a Department of Chemistry, Hong Kong Baptist University. Waterloo Rd, Kowloon, Hong Kong, China.

b Department of Biomedical engineering, Tufts University, 4 colby, Medford, MA 02155, USA.

Computational fluid dynamics (CFD) simulations

We employed computational fluid dynamics (CFD) simulations to design a 3-D shaped chamber in the middle of the channel to reduce the shear rate and facilitate the attachment of bacteria. Six different sizes of the deepened wells in the 3-D shaped chamber were designed and tested in CFD simulations (**Tab. S1**). The simulation is based on Naiver-Stokes equation. The inner surface of channel is assumed to be non-slip. The simulation results of the average shear rates at the bottom of the wells are shown in **Fig. 2a&b**.

Table S1. Different sizes of the deepened chamber (μm).

Channel		**Upper chamber**			**Deepened chamber**		
Hight	Width	Hight	Semi major axis	semi minor axis	Hight	Semi major axis	semi minor axis
50	100	50	4000	2000	80	4000	2000
						3500	1750
						3000	1500
						2500	1250
						2000	1000
						1500	750

Operating procedure of AST on our microfluidic platform

At the beginning of a test, the bacteria were injected through Inlet 3; the injection of the bacteria was monitored under fluorescence microscope. After the bacteria were inoculated in the cultivation chambers, antibiotic-doped media and media alone were injected into inlet 1 and inlet 2, respectively (**Fig. S1**). The microfluidic device was placed on a thermostat platform and the bacteria were cultured in the drug concentration gradient at 37 ℃ for 1-2 h.

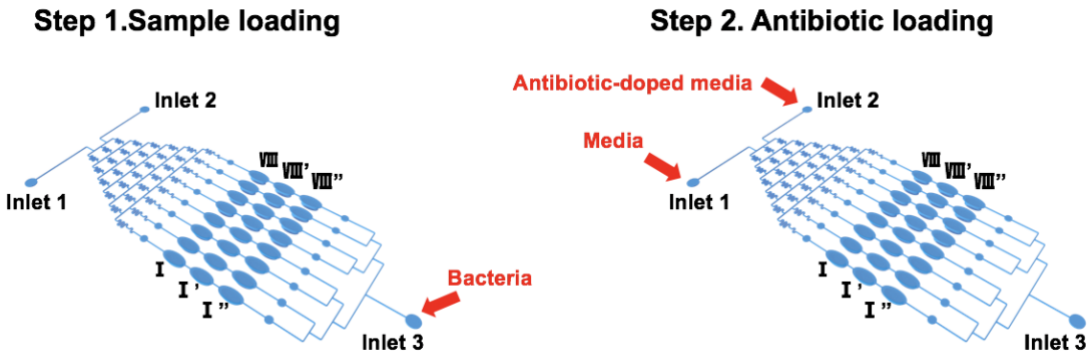

Fig. S1 Operating procedure of AST on our microfluidic platform.

Comparison among polystyrene (PS), PMMA, and PP on solvent resistance and antifouling

Both PS and PMMA have serious problems in solvent resistance and antifouling compared with PP (**Fig. S2, Tab. S2**).

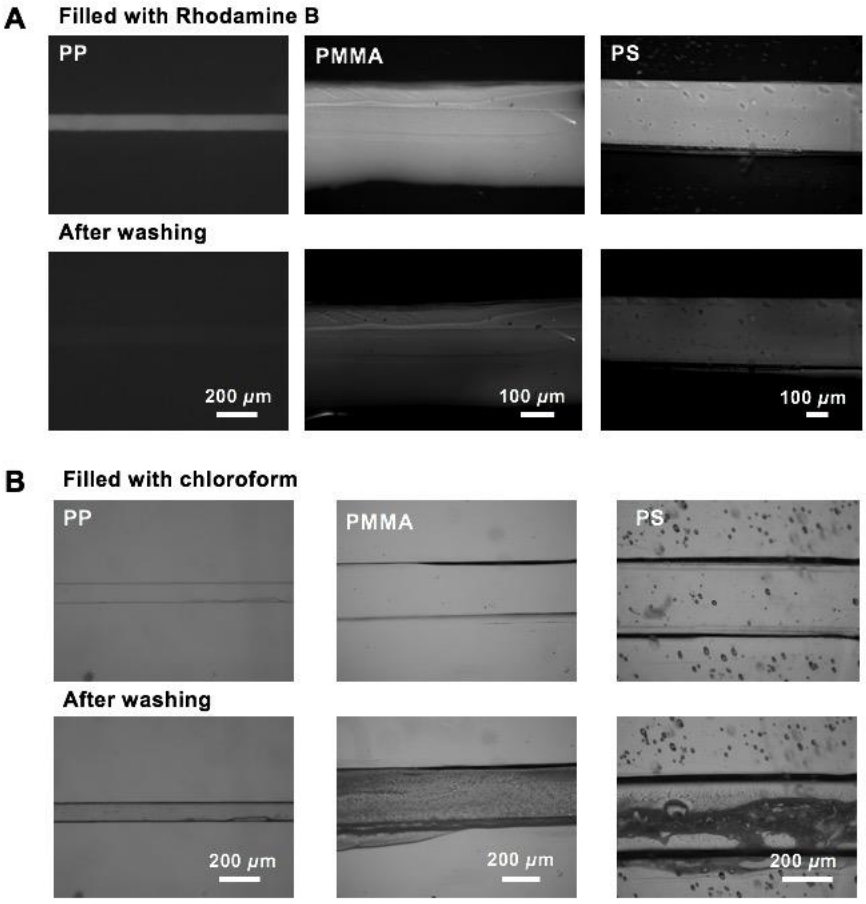

Fig. S2 Comparison among polystyrene (PS), PMMA, and PP on (A) antifouling and (B) solvent resistance tests.

Table. S2 Comparison among the materials of PP, PMMA, PS and PDMS

Property	Polypropylene (PP)	PMMA	Polystyrene (PS)	Polydimethylsiloxane (PDMS)
Anti-fouling	good	moderate	moderate	bad
Optical transparency	moderate	high	high	high
Permeability to air	low	low	low	good
Solvent compatibility	good	moderate (e.g., incompatible with chloroform, methylbenzene, acetone, dimethylbenzene)	moderate (e.g., incompatible with chloroform, methylbenzene, acetone, dimethylbenzene)	bad
Reusability	good	bad	bad	bad
Autoclave sterilization	good	bad	bad	bad

Comparison between our thermally treated PDMS mold and conventional hot embossing mold

Different from conventional hot embossing, we used a thermally treated PDMS as template to mold the PP slides. When using traditional soft molding method, the molded PP slides were unsatisfactory with lots of air bubbles (**Fig. S3**).

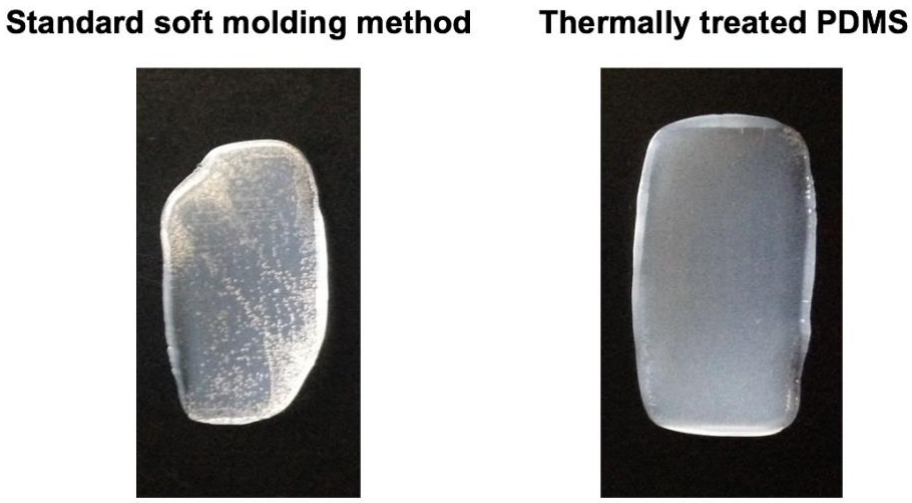

Fig. S3 PP slides molded by two different methods. PP slide with air bubbles molded by standard soft molding method (left); PP slide without air bubbles molded using thermally treated PDMS in our method (right).

Geometry comparison between the thermally treated PDMS mold and the fabricated PP structure

Our method introduces a specially treated thermosetting master (casted at mild temperatures and then used at elevated temperatures) as intermediate, which overcomes the gap between low-melting point master (e.g., photoresist) and high-melting-point replica, therefore effectively solves the problem in microfabricating high-melting-point thermoplastics. The PDMS master became tough enough to withstand noticeable deformation under a pressure of 0.24 MPa due to PDMS component degradation after thermal treatment (**Fig. S4**).

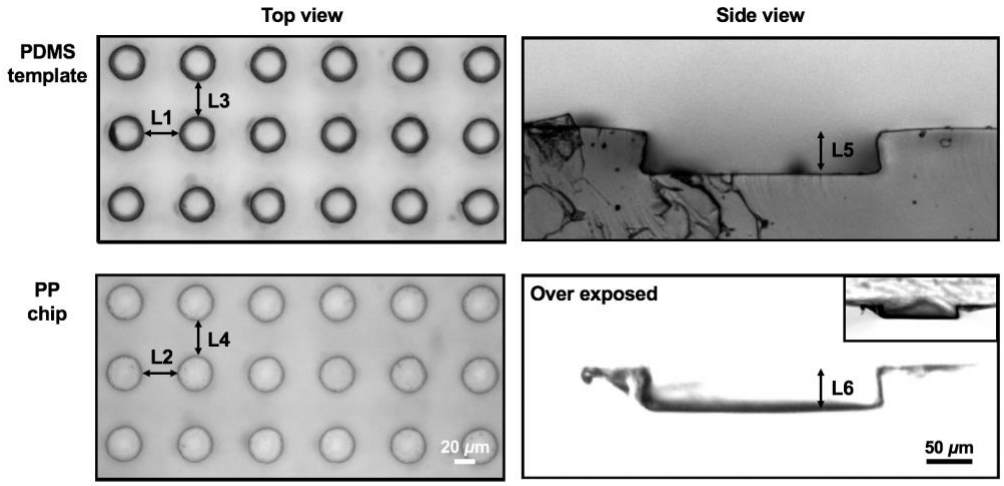

	L1	L2	L3	L4	L5	L6
Length (μm)	34.0	34.0	34.0	34.0	43.5	43.5

Fig. S4 Geometry comparison between the thermally treated PDMS mold and the fabricated PP structure. The pattern on the thermally treated PDMS mold and the replica on fabricated PP chip were highly matched.

High resolution structures based on PP material achieved using our fabrication method

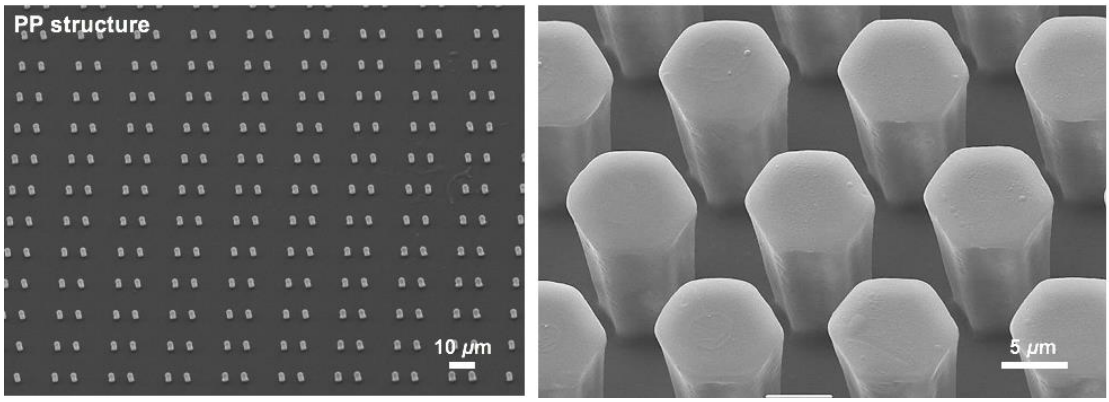

Fig. S5 High resolution structures based on PP material achieved using our fabrication method.

High resolution structures based on PP material achieved using our fabrication method

The coefficients of linear thermal expansion (10^{-6}/K) for steel and PP are around 12 and 80, respectively. When two PP slides are sandwiched within a rigid steel clamp, thermal expansion of the PP will be greater than that of the steel, causing a pressure to build spontaneously. And such pressure is self-regulated as it will automatically reduce with the deformation of the PP slides. According to calculation based on the difference of thermal expansion coefficients between steel and PP as well as the change in temperature during the fabrication (from room temperature to 180 degrees Celsius), the vertical deformation of the chip structure will be about 1% ((80-12)x10-6x (180-20) x100% = 1%) when such pressure reduces to zero. In addition, we measured the height of the channel before and after bonding, the results were good (**Tab. S3**).

Tab. S3 Height of the channel before and after bonding

	Before bonding	After bonding	Difference (%)
Height of the channel (μm)	43.4	43.0	0.92
	54.9	54.3	1.09

Transparency test of different thickness of PP slides

In general, the transparency of PP is considered lower than that of PDMS, limiting its use for making chips for single cell observation. Considering the demand of the visibility of the PP chip under microscope, the absorbance measurement of different thickness of PP slides was performed; it was found that the transmittance of PP is highly related to its thickness (**Fig. S6**). Hence, we used a thin PP slice which is highly transparent for the bonding process.

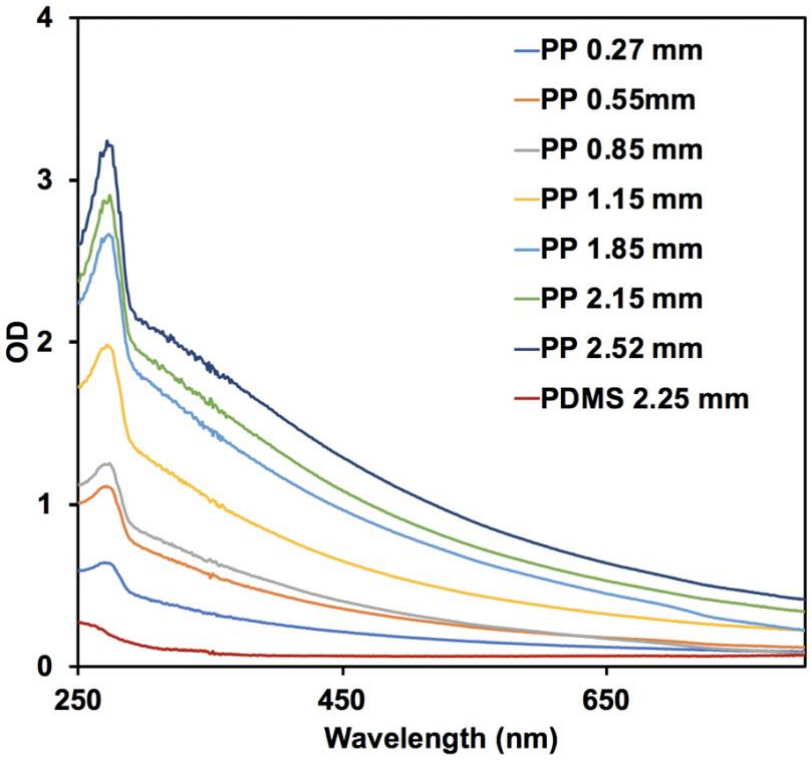

Fig. S6 Absorbance measurement of different thickness of PP slides, compared with a PDMS slide.

Anti-fouling property test of both PP chip and PDMS chip

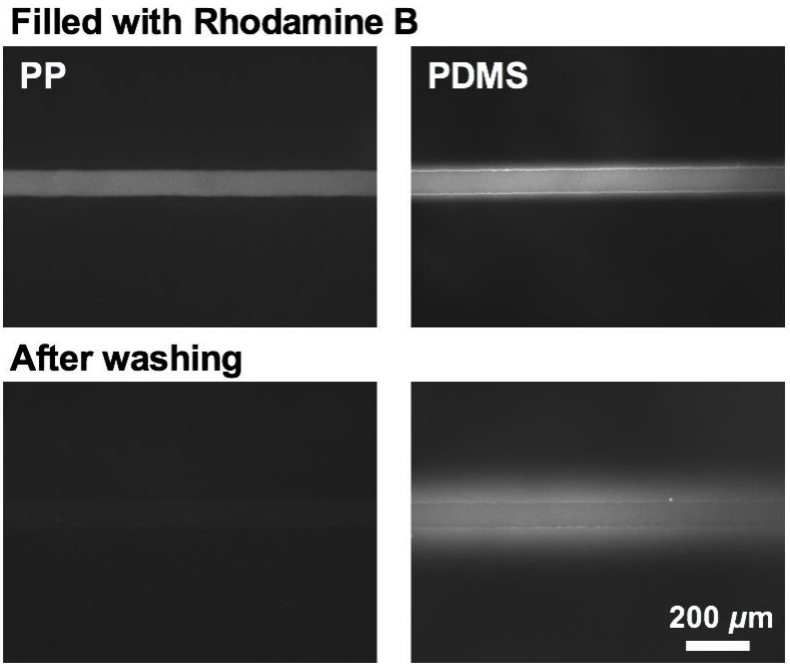

Fig. S7 Antifouling property test of rhodamine B on the PP and PDMS chips. Fluorescence images of channels filled with a 100 μg/mL rhodamine B solution (top), and fluorescence images of the channels after washing with water for 1 min (bottom). The anti-fouling property of the PP chip is observed to be better than that of the PDMS chip. The scale bar represents 200 μm.)

AST experiment of clinical samples on both PP chips and microdilution-based method

Early morning midstream urine samples were collected in 15-mL sterile tubes. Quantitative analyses of urine cultures were performed using the standard calibrated loop method. Urine sample were streaked on Columbia agar with 5% sheep blood and CLED (cysteine-, lactose-, and electrolyte-deficient) agar. Two clinical bacterial strains (*E. coli* and *S. aureus*) were isolated from urine samples, which were provided by the Eighth Affiliated Hospital of Sun Yat-sen University, Shenzhen, China.

Because the bacterial samples were de-identified before we received them, this study was exempted from human subjects research review. The clinical bacterial strains (*E. coli* and *S. aureus*) were pre-activated in an incubator for 15 min under 37 °C before use and injected from the inlet of the microfluidic device at the downstream side; the injection of the bacteria was monitored under microscope. After the bacteria were inoculated into the cultivation chambers, the microfluidic device was placed on a thermostat platform and incubated at 37 °C for 1-2 h. The MIC value was judged by the cell density and the morphology change of the bacteria after incubation; computer software named ImageJ 1.4 was used for the cell counting function. The AST results were consistent with those determined by the hospital's clinical microbiology laboratory using microdilution-based method; while our method provides quantitative results, the latter only provide qualitative results (**Tab. S4**).

Tab. S4 AST results of clinical samples on the PP chips comparison with the results obtained from the hospital clinical microbiology laboratory.

	MIC of *E. coli* - PP Chip (μg/mL)		MIC of *S.aureus* - PP Chip (μg/mL)		MIC of *E. coli* - clinical results (μg/mL)		MIC of S.aureus – clinical results (μg/mL)	
	sample 1	sample 2	sample 1	sample 2	sample 1	sample 2	sample 1	sample 2
Ampicillin	Resistant	1-1.5	-	-	>=32	<=2	-	-
Gentamicin	0.5-0.75	0.5-0.75	0.25-0.5	0.25-0.5	<=1	<=1	<=0.5	<=0.5
Tetracycline	-	-	Resistant	0.6-0.8	-	-	>=16	<=1
Erythromycin	-	-	Resistant	0.1-0.2	-	-	>=8	<=0.25

Reusability performance of our PP chip for AST.

In order to illustrate the potential of commercialization for our AST device, a same chip was used to carry out AST experiments of different antibiotics alternatively for *E. coli* (**Fig. S8**); and a same chip was used to test each type of antibiotic for *S. aureus* (10 times) (**Fig. S9**). No deviation was observed in the results; the MIC values of the under different antibiotics were obtained in accordance with the data from CLSI.

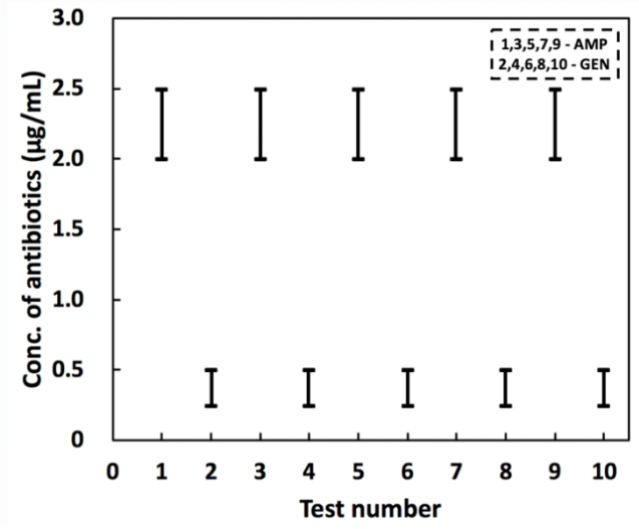

Fig. S8 Reusability performance of our PP chip for AST. The same chip was used to carry out AST experiments of two antibiotics alternatively on *E. coli* for 10 times; odd-number tests were with ampicillin (AMP) and even-number tests were with gentamicin (GEN).

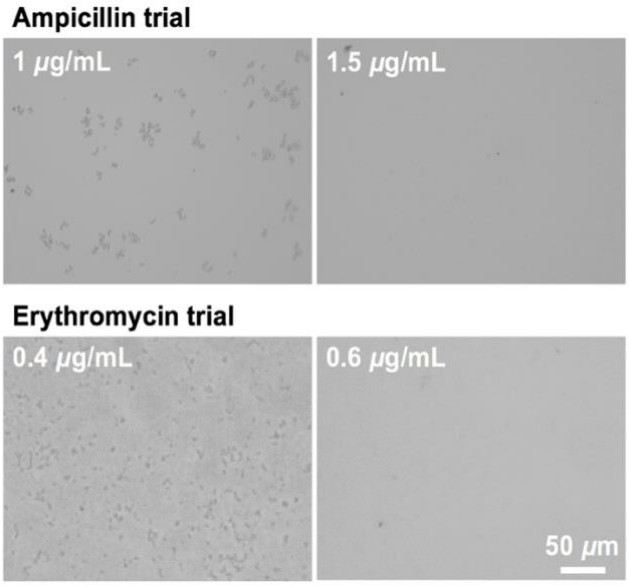

Fig. S9 Microscopic images for the test of MIC value with antibiotics based on different mechanisms (*S.aureus*). The scale bar represents 50 μm.